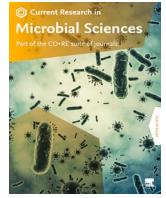



Contents lists available at [ScienceDirect](https://www.sciencedirect.com)

Current Research in Microbial Sciences

journal homepage: www.sciencedirect.com/journal/current-research-in-microbial-sciences

Interrelationship between altered metabolites and the gut microbiota in people living with HIV with different immune responses to antiretroviral therapy

Xuebin Tian^{a,b}, Zhongyao Gao^c, Yiwen Xie^{a,b}, Xiangyun Lu^b, Yulong Zhao^d, Peng Yao^e, Mingqing Dong^e, Lifeng Yu^{f,*}, Nanping Wu^{a,b,*}

^a Cell Biology Research Platform, Jinan Microecological Biomedicine Shandong Laboratory, Jinan, Shandong, China

^b State Key Laboratory for Diagnosis and Treatment of Infectious Diseases, National Clinical Research Center for Infectious Diseases, National Medical Center for Infectious Diseases, Collaborative Innovation Center for Diagnosis and Treatment of Infectious Diseases, The First Affiliated Hospital, Zhejiang University School of Medicine, Hangzhou, Zhejiang, China

^c College of Life Sciences, Wuhan University, Wuhan, Hubei, China

^d Shandong First Medical University, Jinan, Shandong, China

^e Department of Infectious Disease, Zhejiang Qingchun Hospital, Hangzhou, Zhejiang, China

^f Department of Critical Care Medicine, The First Affiliated Hospital of Shandong First Medical University & Shandong Provincial Qianfoshan Hospital, Shandong medicine and Health Key Laboratory of Emergency Medicine, Shandong Institute of Anesthesia and Respiratory Critical Medicine, Jinan, Shandong, China

ARTICLE INFO

Keywords:

Human immunodeficiency virus
Gut microbiota
Fecal metabolites
Immunological responders
Immunological non-responders

ABSTRACT

Background: Antiretroviral therapy (ART) effectively reduces opportunistic infections and mortality in people living with HIV (PLWH); however, some patients exhibit poor immune recovery. This study explores the connections among immune responses, metabolites, and the gut microbiota in PLWH with differing reactions to ART. **Methods:** We analyzed the gut microbiota composition, metabolites, and immune markers in 38 PLWH who showed an immunological response (IR) and 32 who did not (INR), as classified according to CD4+ T-cell levels after 24 months of ART. Additionally, in vitro assays using cell counting kit 8, flow cytometry, and quantitative real-time reverse transcription PCR were employed to assess the effects of the metabolites on cell viability, immune marker expression, and cytokine levels.

Results: Gut microbiota and metabolic profiles differed significantly between the IR and INR groups. *Enterococcus* was more abundant in the INR group, whereas [*Ruminococcus*]*gnavus* group levels were reduced. Significant metabolic pathway alterations included decreased folate biosynthesis and biotin metabolism. We observed negative associations of *Parabacteroides* with activation markers on CD4+ T-cells, and positive correlations with CD4/CD8 ratios. *Enterococcus* showed inverse relationships with these markers. Indole-3-acetyl-beta-1-D-glucoside (area under the curve value = 0.8931), had the best discriminatory ability. Further experiments showed that Indole-3-acetyl-beta-1-D-glucoside significantly decreased the proportions of CD4+CD57+, effector CD4+, CD4+PD1+, CD8+CD57+, effector CD8+, and CD8+HLA-DR+ T cells. Moreover, mRNA expression analysis showed that Indole-3-acetyl-beta-1-D-glucoside treatment led to a suppression of pro-inflammatory cytokines.

Conclusion: The multi-omics approach highlighted potential biomarkers for immune recovery in HIV, suggesting avenues for further research into treatment strategies.

Introduction

Plasma human immunodeficiency virus (HIV) RNA levels are effectively suppressed to undetectable levels by antiretroviral therapy (ART), thereby facilitating immune system recovery. This crucial intervention

significantly diminishes the risk of opportunistic infections and increases the survival rate in people living with HIV (PLWH) (Davenport et al., 2019; Sun et al., 2017). However, in contrast to immunological responders (IRs), certain PLWH cannot achieve CD4+ T-cell count normalization even after continued virological suppression, and are thus

* Corresponding author.

E-mail addresses: 13964095762@139.com (L. Yu), flwnp2013@163.com (N. Wu).

<https://doi.org/10.1016/j.crmicr.2025.100340>

Available online 10 January 2025

2666-5174/© 2025 The Authors. Published by Elsevier B.V. This is an open access article under the CC BY-NC-ND license (<http://creativecommons.org/licenses/by-nc-nd/4.0/>).

termed immunological non-responders (INRs), who have a heightened risk of fast disease progression and increased mortality (Xie et al., 2021).

In the human body, the biggest microbial community is the gut microbiota (Lloyd-Price et al., 2017; de Vos et al., 2022). The gut microbiota exerts an important function by regulating host processes, including dietary fiber fermentation, metabolism, and immune maturation (Simpson and Campbell, 2015; Nogal et al., 2021; Zheng et al., 2020). Xie et al. investigated the relationships between the microbiota and different immune responses to ART in PLWH (Xie et al., 2021; Xie et al., 2021). However, such genomic level analysis reveals only the microbial make-up and potential of the gut microbiota, but not their activities. Moreover, the interrelationships among the host, diet, and the gut microbiota cannot be determined by genomics alone.

Metabolomics is a powerful tool to explore disease mechanisms. Host and gut microbiota-produced metabolites support the physiology and stability of the gut microenvironment. Metabolites associated with the gut microbiota (such as tryptophan metabolites, bile acids, or short-chain fatty acids [SCFAs]) affect the immunoregulation and metabolic homeostasis of the host (Bunnnett, 2014; Jeong et al., 2023). Qian et al. investigated the association between plasma metabolite profiles and immune recovery in IRs and INRs following ART (Qian et al., 2021). Nevertheless, limited information is available regarding the interrelationships among immune markers, gut metabolites, and the gut microbiota in IRs and INRs.

Herein, we integrated 16S rRNA gene sequencing and liquid chromatography-mass spectrometry (LC-MS) untargeted metabolomics, aiming to determine the associations among the immune response, metabolites, and the gut microbiota. This information might lead an increased comprehension of the communication between the host and the gut microbiota and the development novel strategies for treatment and intervention.

Materials and methods

Study participants

Seventy PLWH (38 IRs and 32 INRs), diagnosed at the Disease Control and Prevention Center of Zhejiang Province, were recruited from the HIV clinic of the First Affiliated Hospital of Zhejiang University (Zhejiang, China) from November 2020 to December 2022. All patients had received ART from the beginning of the chronic phase of HIV infection. Herein, we defined IRs and INRs as patients with an average of the last two CD4+ T-cell counts/ $\mu\text{L} \geq 500$ (IRs) or < 200 (INRs) after 24 months of receiving ART. All patients had achieved undetectable viral loads, defined as < 20 copies/mL, after 24 months of ART, confirming successful viral suppression in all participants. Subjects were provided individually with information about the study, especially the risks and benefits. The participants provided written informed consent. We excluded those who received probiotics, antibiotics, or both within 4 weeks before enrollment. This study was approved by the Institutional Review Committee of the First Affiliated Hospital of Zhejiang University (ethical number 2020-IIT54). Written informed consent was obtained from all participants. All methods adhered to the relevant guidelines set by the institutional ethics committee.

Collection of blood collection and analysis of cytokines

Samples of plasma were collected into 10 mL vacutainers. The blood samples were mixed well and subjected to centrifugation at $3000 \times g$ for 10 minutes to collect the plasma (supernatant), which was placed at -80°C . Cytokine levels were determined using a Meso Scale Discovery (MSD, Rockville, MD, USA) electrochemiluminescence V-PLEX assay, including interferon (IFN)- γ , tumor necrosis factor alpha (TNF- α), interleukin (IL)-22, IL-21, IL-17F, IL-17A, IL-13, IL-12p70, IL-10, IL-9, IL-8, IL-6, IL-5, IL-4, IL-2, and IL-1 β (pg/mL). Two-fold diluted plasma samples were determined in duplicate. The cytokine concentrations

were determined using attached electrochemiluminescent labels on plates in the MSD apparatus (MESO QuickPlex SQ 120). Variations between plates were determined by including high and low level controls, giving an inter-assay coefficient of variation of $< 10\%$. MSD Discovery Workbench analysis software was used to analyze the results.

Cell counting kit-8 (CCK-8) assay

The experiment included a blank group, a control group, and several groups treated with different concentrations of metabolites. Peripheral blood mononuclear cells (PBMCs) were seeded in a 96-well plate at a density of 5×10^3 cells per well and cultured for 24 hours. Each group was set up with three replicate wells. The CCK-8 solution (Catalog No. HY-K0301, MCE, Monmouth Junction, NJ, USA) was mixed with minimal essential medium (MEM) culture medium containing metabolites at a ratio of 1:9. The samples were then incubated at 37°C in the dark for 2 hours. The optical density at 450 nm (OD450) was measured using a microplate reader (Molecular Devices, San Diego, CA, USA). The average values were calculated, and a survival rate curve was plotted.

Quantitative real-time reverse transcription PCR (RT-qPCR) analysis

Total RNA was extracted using a Super FastPure Cell RNA Isolation Kit (Catalog No. RC102, Vazyme, Nanjing, China) according to the manufacturer's instructions. Reverse transcription was performed using a ReverTra Ace qPCR RT Kit (Catalog No. FSQ-301, TOYOBO, Tokyo, Japan) to synthesize complementary DNA (cDNA). The qPCR reaction was carried out using a THUNDERBIRD® Next qPCR Mix (Catalog No. QPX-201, TOYOBO) on a Bio-Rad CFX96 Real-Time PCR System (Bio-Rad, Hercules, CA, USA) with the following conditions: 95°C for 30 seconds, followed by 40 cycles of 95°C for 5 seconds and 60°C for 30 seconds. Relative gene expression levels were calculated using the $2^{-\Delta\Delta\text{Ct}}$ method (Livak and Schmittgen, 2001), with *ACTB* (encoding β -actin) serving as the reference gene. The primers used in this study are listed in Table S1.

Flow cytometry and immunophenotype

Supplementary Table S2 lists the reagents used. According to the manufacturer's instructions (BD Biosciences, San Jose, CA, USA), PBMCs were isolated from whole blood using Ficoll density gradient centrifugation. Viable cells were identified using a live/dead stain (Fixable Viability Stain 510, 1:1000, BD Biosciences). After washing with fluorescence activated cell sorting (FACS) buffer (Stain buffer, BD Biosciences), staining was carried out at 4°C for 30 min employing fluorescently labeled antibodies at 1:100 dilution: anti-human CD3, anti-human CD4, anti-human CD8, and anti-human T cell receptor (TCR) $\gamma\delta$, anti-human CD25, anti-human CD127, anti-human CD45RA, anti-human CD62L, anti-human leukocyte antigen-DR isotype (HLA-DR), anti-human CD28, anti-human CD57, and anti-human CD279 (all purchased from BD Biosciences). Thereafter, the cells were washed again, followed by suspension in 200 μL of FACS buffer. The cells in the samples were determined on a CytoFLEX LX flow cytometer (Beckman Coulter, Inc., Brea, CA, USA), with data analysis carried out using FlowJo software version 10.10.0 (Treestar Inc., Ashland, OR, USA).

High-throughput sequencing of 16S rRNA

An Omega Mag-Bind Stool DNA kit (Omega Bio-Tek, Norcross, GA, USA) was employed to isolate total DNA from collected fecal samples. Polymerase chain reaction (PCR) was carried out to obtain the V3-V4 variable region of the 16S rRNA gene from the bacterial genomes using the forward primer 5'-ACTCCTACGGGAGGAGCA-3' and reverse primer 5'-GGACTACHVGGGTWTCTAAT-3'. An Illumina TruSeq Nano DNA LT library prep kit (Illumina, San Diego, CA, USA) was employed to construct the sequencing library, which was sequenced on the Illumina

platform. The obtained sequences were optimized using dada2 in the Quantitative Insights into Microbial Ecology2 (QIIME2) software (v2019.4) (Caporaso et al., 2010). QIIME2 was also used to allocate the taxonomy of representative sequences by querying the Greengenes database (<http://greengenes.secondgenome.com/>) with default settings. Species annotation was carried out using the pretrained naive Bayes classifier (<https://github.com/QIIME2/q2-feature-classifier>) (DeSantis et al., 2006; Bokulich et al., 2018).

Liquid chromatography-mass spectrometry

We extracted metabolites from pretreated fecal samples. A Vanquish ultrahigh performance liquid chromatography (UHPLC) System (Thermo Fisher Scientific, Waltham, MA, USA) was employed for LC analysis.

An ACQUITY UPLC HSS T3 column (150 × 2.1 mm, 1.8 μm; Waters, Milford, MA, USA) was employed for chromatography. The temperature of the chromatographic column remained at 40 °C in the mobile phase, maintaining a flow rate of 0.25 mL/min. The mass spectrum condition was electrospray ionization (ESI), acquiring signals in positive and negative ion scanning modes. In positive ion mode, the mobile phase comprised (C) 0.1% formic acid in acetonitrile (v/v) and (D) 0.1% formic acid in water (v/v), while in negative ion mode, the mobile phase was (A) acetonitrile and (B) ammonium formate (5 mM). The scanning range comprised 100–1000 m/z (Zelena et al., 2009).

Statistical and bioinformatic analyses

Central tendency (a single value summary statistic describing a dataset, reflecting the center of its distribution) was measured according to geometric mean (GM) values. The differences between the INR and IR groups were assessed employing the Mann–Whitney test incorporating Holm’s correction for multiple comparisons. Categorical variables were assessed employing Fisher’s exact test. Significantly differentially abundant microbiota and differentially abundant microbiome members were screened and analyzed employing linear discriminant analysis (LDA) effect size (LEfSe), with selection according to an LDA-value > 4. Phylogenetic Investigation of Communities by Reconstruction of Unobserved States 2 (PICRUST2) from the Kyoto Encyclopedia of Genes and Genomes (KEGG) database was employed to carry out KEGG Orthology (KO) analysis and predict the functions of microbes. Differences between the two groups were assessed using Orthogonal partial least-squares discriminant analysis (OPLS-DA). Associations between differentially abundant bacteria and the relative levels of the top 50 differentially abundant fecal metabolites were assessed using Spearman correlation analysis. All statistical determinations were carried out in R (version 4.2.1) (Team., 2020). A *P* value < 0.05 was considered statistically significant. To assess the discriminatory accuracy of the differentially abundant genera and metabolites, we constructed a receiver operating characteristic curve (ROC) to determine the area under the curve (AUC).

Results

Participant characteristics

The was a cross-sectional study that included 38 IR and 32 INR PLWH. The two groups were relatively matched for sex, smoking status, age, and ongoing ART regimen (Table 1). As expected, the IR group had a significantly higher nadir and current CD4+ T cell counts and CD4/CD8 ratios than the INR group (*P* < 0.001). All patients had undetectable (< 20 copies/mL) HIV RNA viral loads. The proportion of CD4+ CD28+, regulatory T cells (Treg) cells, CD8+ CD25+, and effector CD8+ T-cells were similar in the IR and INR groups (Table S3). Of the 16 markers studied, the groups showed no differences in the levels of IFN-γ, IL-13, IL-1β, IL-4, IL-5, IL-9, IL-17F, and IL-21, while the levels of remaining 8 markers (IL-10, IL-12p70, IL-2, IL-6, IL-8, TNF-α, IL-17A,

Table 1

Clinical characteristics of the study cohort.

Characteristics	HIV(+) Cases		<i>P</i> value
	Immune Responders (IRs)	Immune Non-responders (INRs)	
Number of patients	38	32	
Gender Male/female	38/0	31/1	0.4571
Age, median (IQR)	42 (34, 45)	44.5 (31, 58.25)	0.1156
Smokers (number)	0	1	0.4571
Nadir CD4 + T cell count, median (IQR)	312 (219, 347)	123.5 (84, 162.3)	<0.0001
Current CD4 + T cell count, median (IQR)	521.5 (421, 754)	102 (60, 174.5)	<0.0001
Current CD4 + /CD8 + T-cell ratio	0.97 (0.80, 1.24)	0.26 (0.14, 0.40)	<0.0001
HIV RNA	ND	ND	
Transmission type (number)			
Heterosexual / Homosexual	7/31	6/26	>0.9999
Ongoing ART regimen, N (%)			
NNRTI-based	36 (94.74%)	28 (87.50%)	0.4016
PI-based	2 (5.26%)	4 (12.50%)	0.4016

Abbreviations: HIV, human immunodeficiency virus; IQR, interquartile range; ND, not detected; MSW, men who have sex with women; MSM, men who have sex with men; NNRTI, non-nucleoside reverse transcriptase inhibitors; PI, protease inhibitor; IR, immunological responders; INR, immunological non-responders.

and IL-22) were significantly different between the two groups (Table S3).

Gut microbiota analysis in the immunological responder and immunological non-responder groups

Venn diagram analysis showed that the IR and the INR groups shared 2081 amplicon sequence variants (ASVs), whereas the IR group had 13,217 unique ASVs and the INR group had 10,051 unique ASVs (Fig. 1A). At the level of phyla, *Firmicutes*, *Proteobacteria*, *Actinobacteria*, and *Bacteroidetes* represented the major members of the gut microbiota (Fig. 1B). At the level of genera, *Escherichia-Shigella* was the most common member in the two groups. The INR group had a higher proportion of *Enterococcus* than the IR group, but a lower proportion of *[Ruminococcus]_gnavus_group* (Fig. 1C).

The IR group had a higher species alpha diversity than the INR group (*P* = 0.025); however, the species richness between groups was not significantly different (*P* = 0.16) (Fig. 1D). Principal-coordinate analysis (PCoA) indicated a large difference in beta diversity between the IR and INR groups (*P* = 0.007), indicating that the groups had differences in their microbiota composition (Fig. 1E). The LDA threshold was set to 4 for LEfSe analysis to examine the significant differences in microbial species between the groups. This analysis identified 23 enriched species (Fig. 1F). As shown in the chart, *Bifidobacteriaceae* and *Bacteroides* were relatively highly abundant in the IR group, while *Enterococcus* was relatively highly abundant in the INR group.

Prediction of the potential functions of the altered microbiome

PICRUST2 was employed to determine KEGG Orthology (KO) level 3 pathways for the functional analysis of the two groups. Glycerophospholipid metabolism and synthesis, and degradation of ketone bodies were significantly increased in the INR group compared with those in the IR group, while folate biosynthesis; biotin metabolism; histidine metabolism; arginine and proline metabolism; and phenylalanine, tyrosine, and tryptophan biosynthesis were increased significantly in the IR group compared with those in the INR group (Fig. 2A).

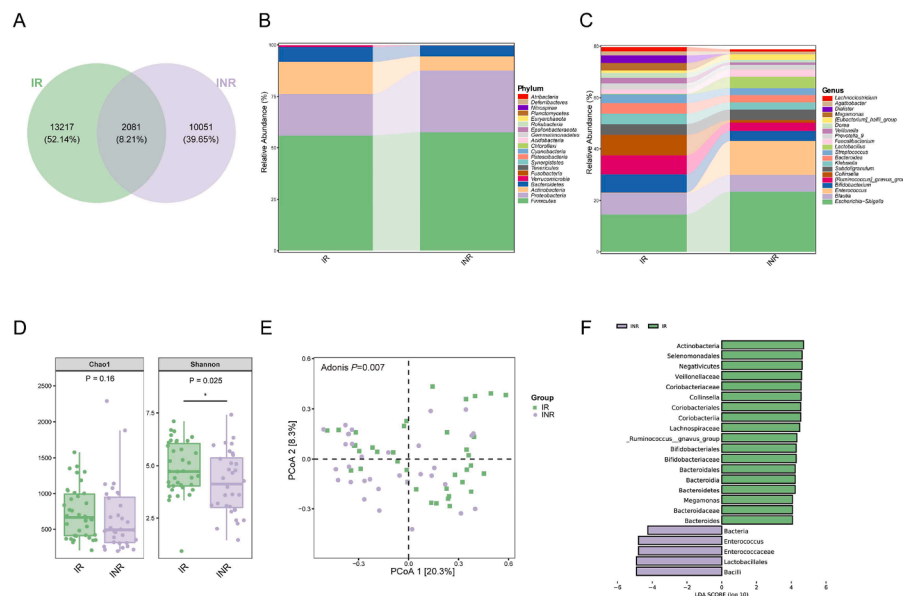


Fig. 1. (A) Venn diagram of the IR group and INR group. (B) Histogram of the phylum level microbiota composition of the IR and INR groups. (C) Histogram of the genus level microbiota composition of the IR and INR groups. (D) Chao1 indices of species richness between the IR and INR groups. Shannon indices of species evenness between the IR and INR groups. (E) PCoA plot indicating the alterations in microbial composition of the feces between the IR and INR groups. (F) LDA score diagram and the significantly differentially abundant genera between the IR and INR groups. The groups are shown in different colors, and the histogram length indicates the LDA score. A higher score represents a more significant difference between the microbiomes of the IR and INR groups (LDA threshold of 4). IR, immune responder; INR, immune non-responder; PCoA, principal-coordinate analysis; LDA, linear discriminant analysis.

IR and INR gut sample metabolomic signatures

To determine the impact of HIV infection on the fecal metabolites of IRs and INRs, we carried out LC-MS untargeted metabolomics. The IR and INR groups were effectively discriminated using OPLS-DA (Fig. S1A), revealing the presence of significant differentially abundant metabolites between the two groups (Fig. S1B). We analyzed 829 fecal metabolites, among which 256 were differentially abundant (Fig. 2B shows the top 50). Compared with those in the IR group, the top 5 differentially abundant metabolites included significant decreases in Indole-3-acetyl-beta-1-D-glucoside, loperamide, Ergosta-5,7,22,24(28)-tetraen-3beta-ol, and luteolin, and significant increases in 2-Dehydropantoate in the INR group (Fig. 2C).

Possible effects of the differentially abundant metabolites on host metabolic pathways

KEGG pathway mapper was then used to annotate the differentially abundant metabolites. Comparisons of the human metabolic profiles indicated significant alterations to central carbon metabolism, protein digestion and absorption, and amino acid pathways (Fig. S2).

Relationships among differentially abundant microbiota, distinct fecal metabolites, and immune markers

To understand the potential correlation among the gut microbiome, fecal metabolites, and immune markers, we performed Spearman correlation analysis (Fig. 3A, B). The analysis revealed a negative correlation between the abundance of *Parabacteroides* and the numbers of CD4+ HLA-DR+ T-cells and CD4+ programmed cell death 1 (PD-1)+ T-cells, but a positive correlation with IL-17A levels. Additionally, *Lachnospirillum* correlated positively with the numbers of CD8+CD28+ T-cells, *Bacteroides* correlated with IL-10 levels, and *Enterococcus* correlated negatively with IL-22 levels. Remarkably, parameters such as the CD4/CD8 ratio, and nadir and current numbers of CD4+ T cells showed a positive association with *Parabacteroides*, but correlated negatively with *Enterococcus*, indicating complex interactions between the gut

microbiota and immune responses (Fig. 3A).

The human KEGG pathway mapper annotated two of top 50 differentially abundant fecal metabolites. We then tabulated the correlations among the differentially abundant fecal metabolites, altered bacteria, and human metabolic pathways (Table S4). The results indicated that two differentially abundant microbiota members and two differentially abundant fecal metabolites were closely related, which might influence particular human metabolic pathways.

Several metabolites showed significant correlations with immune markers. Notably, metabolites such as 2-Deoxy-scylo-inosose, Indole-3-acetyl-beta-1-D-glucoside, Propafenone, N-Acetyl-leucine, N-Acetyl-beta-glucosaminylamine, and 8,9-DiHETrE, demonstrated notable correlations with T-cell activation markers (e.g., HLA-DR, PD-1) and naive CD4, naive CD8, nadir CD4, and current CD4. Specifically, these metabolites correlated negatively with CD4+ T-cell activation markers (HLA-DR, PD-1), and positively with naive CD4 and CD8 T-cell counts, as well as nadir CD4 and current CD4 levels (Fig. 3C).

Furthermore, the AUC values of the differentially abundant genera and metabolites were determined (Spearman's r -value > 0.5; Fig. 3D). The results showed that to distinguish the IRs and INRs, these genera and metabolites in combination had an AUC value of 0.8125, suggested that the interplay among them was important in the pathogenesis of the different immune responses to ART and are worthy of deeper investigation. In addition, the AUC values of these five genera (*Enterococcus*, [*Ruminococcus*] *gnavus* group, *Bacteroides*, *Ralstonia*, and *Sellimonas*) and five metabolites (Indole-3-acetyl-beta-1-D-glucoside, Loperamide, 2-Dehydropantoate, Ergosta-5,7,22,24(28)-tetraen-3beta-ol, and Luteolin) were calculated to determine the key metabolites or genera. Most of the differentially abundant metabolites had better predictive functions than the differentially abundant genera (Tables S5, S6, and Fig. S2). In particular, Indole-3-acetyl-beta-1-D-glucoside (AUC-value = 0.8931), had the best discriminatory ability. Experiments were conducted to validate the functional effects of Indole-3-acetyl-beta-1-D-glucoside. Based on the results of the CCK-8 assay, Indole-3-acetyl-beta-1-D-glucoside at 2 μ M was selected for further analysis (Fig. S4). Subsequent analyses revealed that treatment with Indole-3-acetyl-beta-1-D-glucoside significantly decreased the proportions of CD4+CD57+,

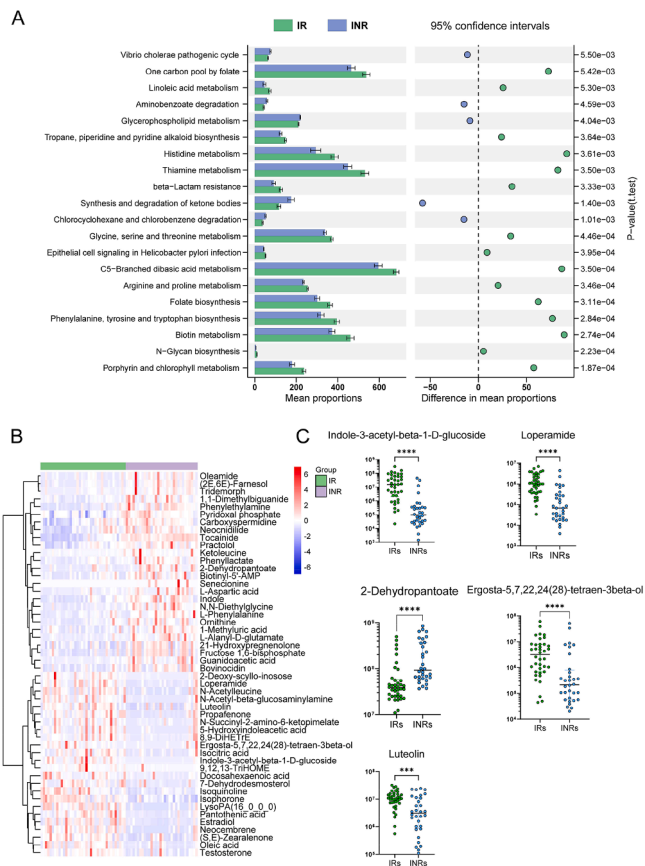


Fig. 2. (A) Predicted microbial functional analysis. Analysis using Phylogenetic Investigation of Communities by Reconstruction of Unobserved States 2 (PIC-RUST2) allowing the identification of Kyoto Encyclopedia of Genes and Genomes (KEGG) Orthology (KO) level 3 pathways between the IR and INR groups. (B) Heat map of the levels of the top 50 differentially abundant metabolites that showed significant changes in the IR vs. INR comparison. (C) Scatter plots of signature metabolites in IRs and INRs. The Y-axis has been placed in a log10 scale. IR, immune responder; INR, immune non-responder.

effector CD4+, CD4+PD1+, CD8+CD57+, effector CD8+, and CD8+HLA-DR+ T cells (Table S7 and Fig.S5). Additionally, in terms of mRNA expression, treatment with Indole-3-acetyl-beta-1-D-glucoside led to reduced levels of IL-6, IL-17A, and IFN- γ (Fig. S6).

Together, our results indicated that being an INR could result in gut dysbiosis, with related effects on human metabolic pathways. The gut microbiota-host interactions resulting from INR status are illustrated diagrammatically in Fig. 4.

Discussion

The host and its microbiota interact dynamically as a critical component of human health (Dethlefsen et al., 2007). It is widely accepted that the gut microbiota functions in maintaining immune balance. Alterations in the composition and function of the gut microbiota have revealed a link between the intestinal bacterial ecosystem and immune responses in individuals with HIV undergoing treatment (Harper et al., 2020; Lujan et al., 2019). Herein, we conducted a comprehensive multi-omics investigation, integrating 16S rRNA transcriptomics and LC-MS untargeted metabolomics, to explore the differences in the gut microbiota composition between IRs and INRs. The major findings included significant disparities in gut microbiota composition between the two groups, and metabolites play a crucial role in immune activation and inflammatory responses.

In agreement with published studies (Xie et al., 2021; Lu et al.,

2021), we showed that, compared with that in the IRs, the gut microbial composition in the INRs exhibited significant alterations. This finding adds to the evidence supporting the pivotal function of the gut microbiota in the immune system, particularly in the context of diseases requiring long-term management. The functional profile of the IR group’s microbiota was significantly higher than that of the INR group, whose gut microbiota revealed a decreasing trend of metabolic function over the course of the disease. The INR group showed significantly decreased predicted microbial functions, such as folate biosynthesis and biotin metabolism. Biotin and folate, as essential B vitamins, are derived from dietary intake through the small intestine and from gut microbiota biosynthesis, with subsequent absorption occurring via the distal gut. These B vitamins serve dual roles as beneficial nutrients and immunoregulators, influencing both bodily functions and the gut microbiota composition (Uebanso et al., 2020). Specifically, folate (vitamin B9) is synthesized by genera such as *Lactococcus spp.*, *Bifidobacterium*, and *Bacteroides*, and crucially functions as a one-carbon unit carrier and donor for DNA synthesis and repair (Kok et al., 2020). Biotin (vitamin B7), produced by *Bacteroides* among others, is integral to various cellular metabolic processes and plays roles in immunological and inflammatory responses (Sirithanakorn and Cronan, 2021).

The differentially abundant metabolites and microbiota members were then subjected to Spearman correlation analysis to gain further details. The analysis showed close correlations between two differentially abundant microbiota members and two differentially abundant fecal metabolites, suggesting their specific impacts on PLWH metabolic pathways. Moreover, our analysis revealed that several metabolites showed significant correlations with immune markers, demonstrating notable correlations with T-cell activation markers and naive CD4, naive CD8, nadir CD4, and current CD4. This suggests a possible role for these metabolites in modulating immune responses, particularly in immune activation and T-cell differentiation.

Our results showed that the differentially abundant genera and metabolites identified herein have undergone significant modifications, suggesting their crucial involvement in the pathogenesis of diverse immune responses to ART. These elements might serve as promising avenues for further investigation into the mechanisms underlying immune recovery in PLWH. In particular, Indole-3-acetyl-beta-1-D-glucoside, Loperamide, and 2-Dehydropantoate, which exhibited AUC-values ≥ 0.8 , demonstrated the highest discriminatory ability, underscoring their potential as pivotal biomarkers. Moreover, the interplay of these microbiota and metabolites, with an AUC-value of 0.8125, was revealed as vitally important to the pathogenesis of different immune responses to ART, meriting further exploration.

Notably, Indole-3-acetyl-beta-1-D-glucoside demonstrated the highest AUC value (0.8931) among the metabolites analyzed, indicating its strong discriminatory ability between the IR and INR groups. This high AUC value suggests that Indole-3-acetyl-beta-1-D-glucoside could serve as a highly effective biomarker to identify immune recovery status in HIV-infected individuals. Further in vitro experiments revealed that Indole-3-acetyl-beta-1-D-glucoside significantly decreased the proportions of CD4+CD57+, effector CD4+, CD4+PD1+, CD8+CD57+, effector CD8+, and CD8+HLA-DR+ T cells. These findings suggest that this metabolite might exert an inhibitory effect on the activation of both CD4+ and CD8+ T cell subsets, indicating its potential role in modulating immune responses. Additionally, mRNA expression analysis showed that Indole-3-acetyl-beta-1-D-glucoside treatment led to a suppression of pro-inflammatory cytokines, which might reflect an anti-inflammatory effect of the metabolite. These results imply that Indole-3-acetyl-beta-1-D-glucoside has the capacity to modulate the immune environment in ways that reduce inflammatory activation, potentially contributing to improved immune regulation in PLWH. This study laid the groundwork for potential clinical applications of Indole-3-acetyl-beta-1-D-glucoside as a biomarker to guide therapeutic strategies aimed at enhancing immune recovery in PLWH.

We identified two differentially abundant bacteria, [*Ruminococcus*]

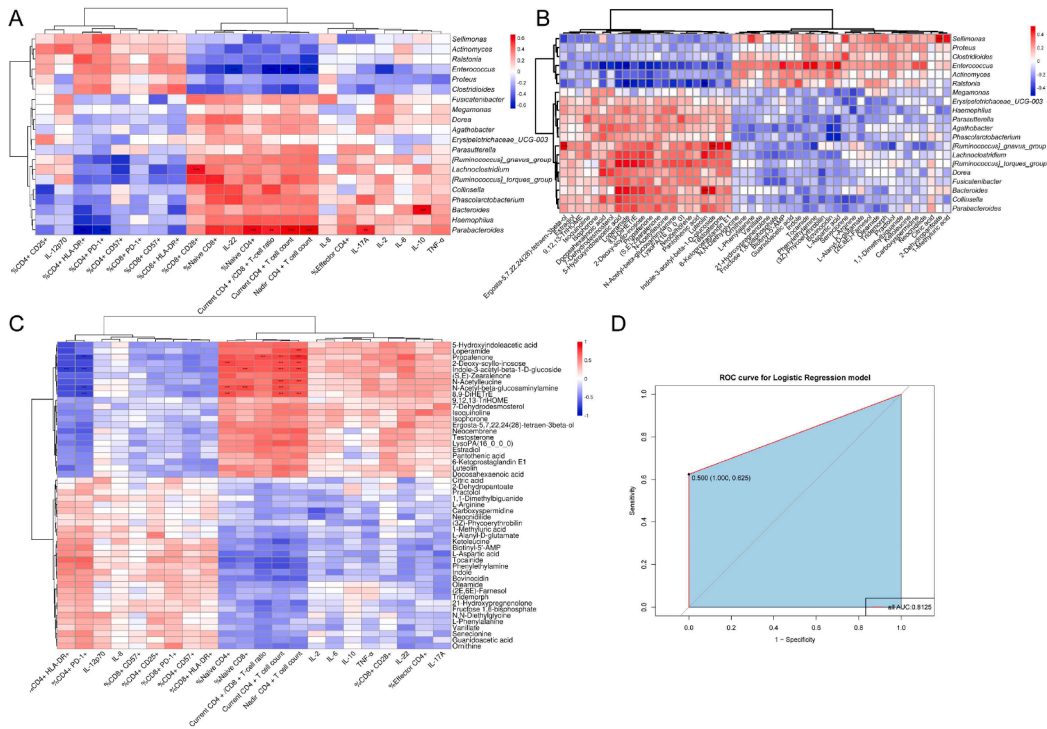


Fig. 3. (A) Heat map of the correlation analysis between immune markers and the fecal microbiota. (B) The top 50 differentially abundant metabolites and bacteria in the IR vs. INR comparison. (C) Heatmap of the correlations between metabolites and immune markers. Correlations based on their relative abundances were analyzed using Spearman correlation analysis. (D) ROC curves of the differentially abundant genera and metabolites combinations that had a Spearman's r -value > 0.5. IR, immune responder; INR, immune non-responder; ROC, receiver operating characteristic curve; AUC, area under the curve; IL, interleukin; HLA-DR, human leukocyte antigen-DR isotype; PD-1, programmed cell death 1; TNF- α , tumor necrosis factor alpha.

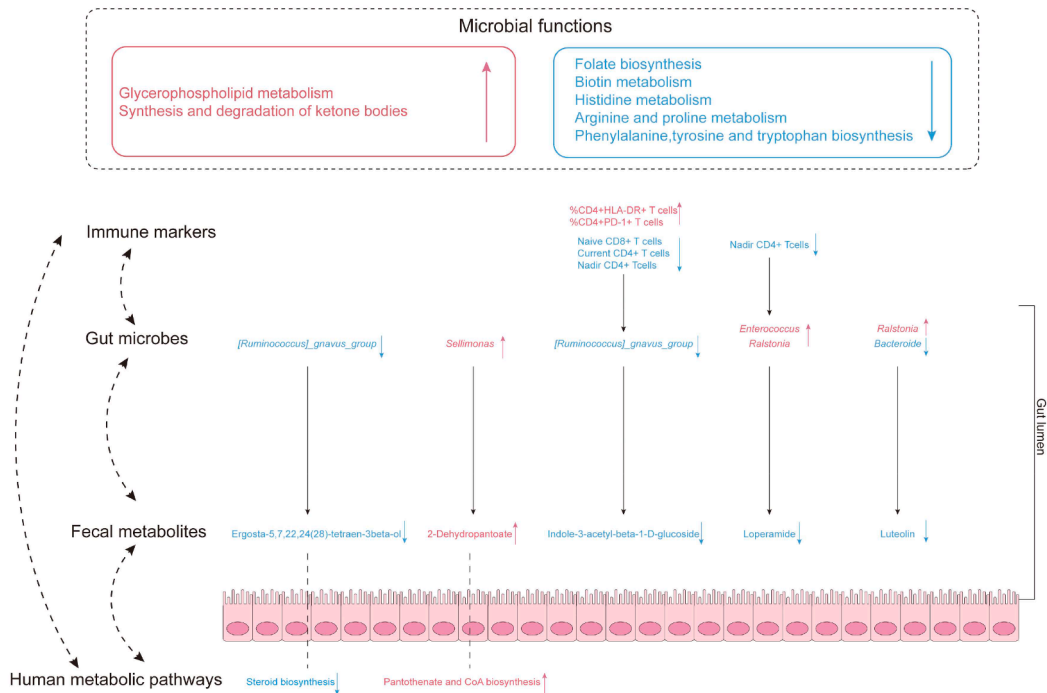


Fig. 4. Diagram showing an overview of the interactions between the host and the gut microbiota in IRs and INRs. Pink and upward arrows indicate upregulated genera, metabolites, and microbial functions in INRs, while blue and downward arrows indicate downregulated genera, metabolites, and microbial functions in INRs.

gnavus_group and *Sellimonas*, which have potential deleterious effects on PLWH. *[Ruminococcus] gnavus_group*, recognized for their mucin-degrading capabilities, are pivotal in early gut colonization, acting as

endogenous nutrient sources. Their capacity to generate SCFAs, tryptophan, and bile acid metabolites underscores their significant metabolic and immunological roles in the gut ecosystem (Croft et al., 2023).

The [*Ruminococcus*] *gnavus* group restrains the secretion of TNF- α and might inhibit the metastasis of lung cancer. In addition, this genus showed a significant correlation with low Alzheimer's disease risk (Ning et al., 2022). Thus, it was hypothesized that INRs are associated with decreased [*Ruminococcus*] *gnavus* group levels. *Sellimonas* shows inflammatory associations and might be upregulated in inflammation-associated diseases, including cirrhosis, atherosclerosis, and ankylosing spondylitis, particularly following gut dysbiosis (Nayfach et al., 2019; Munoz et al., 2020). *Sellimonas* might have an important function in sustaining intestinal homeostasis via metabolic regulation (Munoz et al., 2020). Furthermore, *Enterococcus* might influence host mucosal integrity and immune responses via inflammation. *Enterococcus*, a member of the *Firmicutes* phylum, has been recognized as an opportunistic pathogen. IL-22, belonging to the IL-10 family, is a critical cytokine for mucosal immunity, playing a significant role in tissue regeneration and the regulation of host defenses at barrier surfaces, including the gut and skin (Ouyang and O'Garra, 2019; Kumazawa et al., 2020). In this study, the negative correlation between *Enterococcus* and IL-22 highlights the potential pathogenic role of *Enterococcus* in undermining mucosal barriers and promoting inflammation. Additionally, the observed negative correlations between *Enterococcus* and the CD4/CD8 ratio and nadir and current CD4+ T-cell numbers further illuminate its potential detrimental influence on immune system dynamics, suggesting that *Enterococcus* might play a significant role in immune dysfunction. Moreover, *Parabacteroides* could be a potential probiotic for PLWH. *Parabacteroides*, known as SCFA producers, provide epithelial cells with energy and have a favorable impact on the intestinal barrier (Cui et al., 2022). Herein, the IR group showed higher levels of *Parabacteroides* than the INR group. *Parabacteroides* were negatively associated with activation markers on CD4+ T-cells, but correlated positively with the CD4/CD8 ratio, and nadir and current CD4+ T-cell numbers, suggesting that *Parabacteroides* might be associated with a favorable treatment outcome.

Herein, we revealed, for the first time, the differences in the interactions between the gut microbiome and the host between IR and INR individuals using a combination of metabolomic and microbiota analyses. The health of INRs might benefit from reducing levels of potential pathobionts (e.g., *Sellimonas* and *Enterococcus*), augmenting the levels of potential probiotics (e.g., [*Ruminococcus*] *gnavus* group and *Parabacteroides*), and reversing the decrease in metabolites (e.g., Indole-3-acetyl-beta-1-D-glucoside) by adjusting their diet or adding nutritional supplements. However, the present study has some limitations. It was an observational study; therefore, we could not determine the causal relationships between HIV status and the gut microbiota. Moreover, we collected samples from already HIV-diagnosed individuals; therefore, the gut microbiota alterations might have contributed to, or were a consequence of, HIV infection. In addition, we did not analyze non-bacterial members of the gut microbiota. Thus, further research is required to verify these findings. This study primarily focused on the overall impact of the varying immune responses on the human metabolome and the gut microbiota, providing hints about the disorders of physiology occurring following different immune responses to ART, as reflected by alterations to the metabolome and gut microbiota.

Conclusion

In summary, integrating 16S rRNA data and LC-MS untargeted metabolomics permitted the interactions between the microbiome and host in individuals exhibiting varying immune responses to ART to be characterized. Our findings indicated that INR status not only disturbs the gut microbiome, but also altered metabolites may play a potential role in immune activation and inflammatory responses. These insights will advance our understanding of the immune recovery in patients with immunodeficiency from different perspectives and explore possible new preventative or treatment initiatives.

Declarations

Data Availability: The raw microbiome data are available in the NCBI database under accession number PRJNA1057804. The raw metabolomics data can be found in the MetaboLights database under study identifier MTBLS9264. All data supporting the findings of this study are included in the manuscript and the supplemental material.

Author contributions

Lifeng Yu and Nanping Wu conceptualized the study. Yiwen Xie, Xiangyun Lu, Yulong Zhao, Peng Yao, and Mingqing Dong assisted with conducting the experiments. Xuebin Tian and Zhongyao Gao analyzed the data. Xuebin Tian drafted and revised the manuscript.

Funding

This work was supported by the Research Project of Jinan Microecological Biomedicine Shandong Laboratory [grant number JNL-2022005B], the Shandong Provincial Laboratory Project [grant number SYS202202], and the National Key R&D Program of China [grant numbers 2023YFC2506000, 2023YFC2506004].

Ethics approval and consent to participate

This study was conducted in accordance with the principles of the Declaration of Helsinki and received approval from the Institutional Review Committee of the First Affiliated Hospital of Zhejiang University (ethical number 2020-IIT54). Written informed consent was obtained from all participants. All methods adhered to the relevant guidelines set by the institutional ethical committee.

Declaration of competing interest

The authors declare that they have no known competing financial interests or personal relationships that could have appeared to influence the work reported in this paper.

Acknowledgments

We extend our gratitude to Suzhou Panomix (<http://www.panomix.com/>) for their support. We also appreciate Ying Huang, Dating Han, Haijing Fu, Xiaodi Zhang, and Wanpeng Yin (the First Affiliated Hospital of Zhejiang University) for their help in sample collection.

Supplementary materials

Supplementary material associated with this article can be found, in the online version, at [doi:10.1016/j.crmicr.2025.100340](https://doi.org/10.1016/j.crmicr.2025.100340).

Data availability

Data will be made available on request.

References

- Bokulich, NA, Kaehler, BD, Rideout, JR, Dillon, M, Bolyen, E, Knight, R, et al., 2018. Optimizing taxonomic classification of marker-gene amplicon sequences with QIIME 2's q2-feature-classifier plugin. *Microbiome* 6 (1), 90. <https://doi.org/10.1186/s40168-018-0470-z>.
- Bunnett, NW., 2014. Neuro-humoral signalling by bile acids and the TGR5 receptor in the gastrointestinal tract. *J. Physiol.* 592 (14), 2943–2950. <https://doi.org/10.1113/jphysiol.2014.271155>.
- Caporaso, JG, Kuczynski, J, Stombaugh, J, Bittinger, K, Bushman, FD, Costello, EK, et al., 2010. QIIME allows analysis of high-throughput community sequencing data. *Nat. Methods* 7 (5), 335–336. <https://doi.org/10.1038/nmeth.f.303>.
- Crost, EH, Coletto, E, Bell, A, Juge, N., 2023. *Ruminococcus gnavus*: friend or foe for human health. *FEMS Microbiol. Rev.* 47 (2). <https://doi.org/10.1093/femsr/fuad014>.

- Cui, Y, Zhang, L, Wang, X, Yi, Y, Shan, Y, Liu, B, et al., 2022. Roles of intestinal Parabacteroides in human health and diseases. *FEMS Microbiol. Lett.* 369 (1). <https://doi.org/10.1093/femsle/fnac072>.
- Davenport, MP, Khoury, DS, Cromer, D, Lewin, SR, Kelleher, AD, Kent, SJ., 2019. Functional cure of HIV: the scale of the challenge. *Nat. Rev. Immunol.* 19 (1), 45–54. <https://doi.org/10.1038/s41577-018-0085-4>.
- de Vos, WM, Tilg, H, Van Hul, M, Cani, PD., 2022. Gut microbiome and health: mechanistic insights. *Gut* 71 (5), 1020–1032. <https://doi.org/10.1136/gutjnl-2021-326789>.
- DeSantis, TZ, Hugenholtz, P, Larsen, N, Rojas, M, Brodie, EL, Keller, K, et al., 2006. Greengenes, a chimera-checked 16S rRNA gene database and workbench compatible with ARB. *Appl. Environ. Microbiol.* 72 (7), 5069–5072. <https://doi.org/10.1128/AEM.03006-05>.
- Dethlefsen, L, McFall-Ngai, M, Relman, DA., 2007. An ecological and evolutionary perspective on human-microbe mutualism and disease. *Nature* 449 (7164), 811–818. <https://doi.org/10.1038/nature06245>.
- Harper, A, Vijayakumar, V, Ouwehand, AC, Ter Haar, J, Obis, D, Espadaler, J, et al., 2020. Viral infections, the microbiome, and probiotics. *Front. Cell Infect. Microbiol.* 10, 596166. <https://doi.org/10.3389/fcimb.2020.596166>.
- Jeong, JJ, Ganesan, R, Jin, YJ, Park, HJ, Min, BH, Jeong, MK, et al., 2023. Multi-strain probiotics alleviate loperamide-induced constipation by adjusting the microbiome, serotonin, and short-chain fatty acids in rats. *Front. Microbiol.* 14, 1174968. <https://doi.org/10.3389/fmicb.2023.1174968>.
- Kok, DE, Steegenga, WT, Smid, EJ, Zoetendal, EG, Ulrich, CM, Kampman, E., 2020. Bacterial folate biosynthesis and colorectal cancer risk: more than just a gut feeling. *Crit. Rev. Food Sci. Nutr.* 60 (2), 244–256. <https://doi.org/10.1080/10408398.2018.1522499>.
- Kumazawa, T, Kotake, K, Nishimura, A, Asai, N, Ugajin, T, Yokozeki, H, et al., 2020. Isolation of food-derived bacteria inducing interleukin-22 in B cells. *Biosci. Microbiota Food Health* 39 (1), 1–9. <https://doi.org/10.12938/bmfh.19-012>.
- Livak, KJ, Schmittgen, TD., 2001. Analysis of relative gene expression data using real-time quantitative PCR and the 2(-Delta Delta C(T)) Method. *Methods* 25 (4), 402–408. <https://doi.org/10.1006/meth.2001.1262>.
- Lloyd-Price, J, Mahurkar, A, Rahnavard, G, Crabtree, J, Orvis, J, Hall, AB, et al., 2017. Strains, functions and dynamics in the expanded Human Microbiome Project. *Nature* 550 (7674), 61–66. <https://doi.org/10.1038/nature23889>.
- Lu, D, Zhang, JB, Wang, YX, Geng, ST, Zhang, Z, Xu, Y, et al., 2021. Association between CD4(+) T cell counts and gut microbiota and serum cytokines levels in HIV-infected immunological non-responders. *BMC. Infect. Dis.* 21 (1), 742. <https://doi.org/10.1186/s12879-021-06491-z>.
- Lujan, JA, Rugeles, MT, Taborda, NA., 2019. Contribution of the microbiota to intestinal homeostasis and its role in the pathogenesis of HIV-1 infection. *Curr. HIV. Res.* 17 (1), 13–25. <https://doi.org/10.2174/1570162X17666190311114808>.
- Munoz, M, Guerrero-Araya, E, Cortes-Tapia, C, Plaza-Garrido, A, Lawley, TD, Paredes-Sabja, D., 2020. Comprehensive genome analyses of *Sellimonas intestinalis*, a potential biomarker of homeostasis gut recovery. *Microb. Genom.* 6 (12). <https://doi.org/10.1099/mgen.0.000476>.
- Nayfach, S, Shi, ZJ, Seshadri, R, Pollard, KS, 2019. Kyrpides NC. New insights from uncultivated genomes of the global human gut microbiome. *Nature* 568 (7753), 505–510. <https://doi.org/10.1038/s41586-019-1058-x>.
- Ning, J, Huang, SY, Chen, SD, Zhang, YR, Huang, YY, Yu, JT., 2022. Investigating casual associations among gut microbiota, metabolites, and neurodegenerative diseases: a mendelian randomization study. *J. Alzheimers. Dis.* 87 (1), 211–222. <https://doi.org/10.3233/JAD-215411>.
- Nogal, A, Valdes, AM, Menni, C., 2021. The role of short-chain fatty acids in the interplay between gut microbiota and diet in cardio-metabolic health. *Gut. Microbes.* 13 (1), 1–24. <https://doi.org/10.1080/19490976.2021.1897212>.
- Ouyang, W, O'Garra, A, 2019. IL-10 family cytokines IL-10 and IL-22: from basic science to clinical translation. *Immunity.* 50 (4), 871–891. <https://doi.org/10.1016/j.immuni.2019.03.020>.
- Qian, S, Chen, X, Wu, T, Sun, Y, Li, X, Fu, Y, et al., 2021. The accumulation of plasma acylcarnitines are associated with poor immune recovery in HIV-infected individuals. *BMC. Infect. Dis.* 21 (1), 808. <https://doi.org/10.1186/s12879-021-06525-6>.
- Simpson, HL, Campbell, BJ., 2015. Review article: dietary fibre-microbiota interactions. *Aliment. Pharmacol. Ther.* 42 (2), 158–179. <https://doi.org/10.1111/apt.13248>.
- Sirithanakorn, C, Cronan, JE., 2021. Biotin, a universal and essential cofactor: synthesis, ligation and regulation. *FEMS Microbiol. Rev.* 45 (4). <https://doi.org/10.1093/femsre/fuab003>.
- Sun, Y, Fu, Y, Zhang, Z, Tang, T, Liu, J, Ding, H, et al., 2017. The investigation of CD4+T-cell functions in primary HIV infection with antiretroviral therapy. *Medicine (Baltimore)* 96 (28), e7430. <https://doi.org/10.1097/MD.0000000000007430>.
- Team. RC, 2020. R: A Language and Environment for Statistical Computing. R Foundation for Statistical Computing, Vienna, Austria. <https://www.R-project.org/>. Accessed.
- Uebanso, T, Shimohata, T, Mawatari, K, Takahashi, A., 2020. Functional roles of B-vitamins in the gut and gut microbiome. *Mol. Nutr. Food Res.* 64 (18), e2000426. <https://doi.org/10.1002/mnfr.202000426>.
- Xie, Y, Sun, J, Hu, C, Ruan, B, Zhu, B., 2021. Oral microbiota is associated with immune recovery in human immunodeficiency virus-infected individuals. *Front. Microbiol.* 12, 794746. <https://doi.org/10.3389/fmicb.2021.794746>.
- Xie, Y, Sun, J, Wei, L, Jiang, H, Hu, C, Yang, J, et al., 2021. Altered gut microbiota correlate with different immune responses to HAART in HIV-infected individuals. *BMC. Microbiol.* 21 (1), 11. <https://doi.org/10.1186/s12866-020-02074-1>.
- Zelena, E, Dunn, WB, Broadhurst, D, Francis-McIntyre, S, Carroll, KM, Begley, P, et al., 2009. Development of a robust and repeatable UPLC-MS method for the long-term metabolomic study of human serum. *Anal. Chem.* 81 (4), 1357–1364. <https://doi.org/10.1021/ac8019366>.
- Zheng, D, Liwinski, T, Elinav, E., 2020. Interaction between microbiota and immunity in health and disease. *Cell Res.* 30 (6), 492–506. <https://doi.org/10.1038/s41422-020-0332-7>.